horticulturae

MDPI

Article

CsSE59 Encoding Invertase/Pectin Methyl Esterase Inhibitor Is a Candidate Gene Conferring the Virescent True Leaf Phenotype in Cucumber

Yuelong Zhou, Liting Liao, Liu Liu, Lingdi Xiao, Zixian Zhou, Yong Zhou, Zhaoyang Hu and Shiqiang Liu *

College of Bioscience and Bioengineering, Jiangxi Agricultural University, Nanchang 330045, China; zhouyl21@jxau.edu.cn (Y.Z.); llt18770156559@163.com (L.L.); liuliugl@sina.com (L.L.); xiaolingdixiao@163.com (L.X.); zixianzhou@163.com (Z.Z.); yongzhou@jxau.edu.cn (Y.Z.); huzhaoyang@jxau.edu.cn (Z.H.)

* Correspondence: lsq_hn306@163.com

Abstract: Leaf color mutants are the ideal materials to study the regulation mechanisms of chlorophyll biosynthesis and chloroplast development or as markers for crop breeding. In this study, we identified a virescent true leaf mutant *se59* from the ethyl methane sulfonate (EMS)-induced mutant lines of cucumber (*Cucumis sativus* L.). The *se59* mutant showed normal cotyledons, but the true leaf displays light green at early growth stage, which can recover normal green later. The *se59* locus was controlled by a single recessive nuclear gene. The grana stacking in the chloroplasts of *se59* decreased significantly, and both the photosynthetic ability and the photosynthetic pigment contents of the *se59* were significantly lower than those of wild type. The results of BSA-seq and genotyping showed that an Invertase/Pectin Methyl Esterase Inhibitor (INV/PMEI) protein encoded by *CsSE59* is a candidate gene for the virescent true leaf mutant. The expression level of *CsSE59* in stem, leaf and root is high. Based on the transcriptome analysis of the first true leaf of *se59* mutant, the expression levels of 17 leaf color related genes changed significantly, suggesting *CsSE59* may regulate virescent true leaf by interacting with some of these genes in cucumber. The identification of *CsSE59* is helpful to clarify the role of INV/PMEI in chloroplast development and to understand the mechanisms of leaf color variation in cucumber.

Keywords: leaf color mutant; virescent leaf; INV/PMEI; cucumber

Citation: Zhou, Y.; Liao, L.; Liu, L.; Xiao, L.; Zhou, Z.; Zhou, Y.; Hu, Z.; Liu, S. *CsSE59* Encoding Invertase/Pectin Methyl Esterase Inhibitor Is a Candidate Gene Conferring the Virescent True Leaf Phenotype in Cucumber. *Horticulturae* **2023**, *9*, 951. https://doi.org/10.3390/horticulturae9090951

Academic Editor: Honghao Lv

Received: 10 July 2023
Revised: 8 August 2023
Accepted: 9 August 2023
Published: 22 August 2023

1. Introduction

Plant leaf color is mainly determined by the content and ratio of chlorophylls and carotenoids. Moreover, mutations in key genes related to chloroplast development, chlorophyll biosynthesis and photosynthesis are the main cause of leaf color phenotypes [1]. The study of leaf color mutants helps to understand the genetic mechanism of photosynthesis, chloroplast development, and degradation [2]. Up to now, many leaf color mutants have been studied, such as rice [3], Arabidopsis [4], wheat [5,6], chili [7], carrots [8], soybean [9], corn [10], and so on. These leaf color variations include virescent, light green, stay-green, albino, xanthan, stripes, and zebra [11]. For example, at least 208 leaf color mutants in rice have been reported, of which more than 150 related genes have been identified in detail [12]. These genes are involved in biosynthesis of ribosome [13], chloroplast biosynthesis and development [14–16], and other related functions.

Virescent leaf is an important and specific type of leaf color-related mutation which shows yellow-green cotyledons or true leaves in the early growth stage, and gradually turns green in the process of leaf growth [17]. Many virescent leaf mutants have been reported in different species. For example, many rice virescent leaf-related genes have been cloned [18–22]. Arabidopsis virescent leaf mutant *vir3* has identified and validated a putative chloroplast metalloprotease as the candidate gene for *vir3* [23].

Cucumber is a vegetable crop widely planted all over the world. In cucumber, the work on genetic mapping or elucidating the regulatory mechanism of leaf color mutations is limited, although 19 leaf color mutants have been identified [24–28]. Moreover, only ten leaf color mutations have been cloned in cucumber. The loss of CsTIC21 function encoding the inner membrane transporter component of cucumber chloroplast leads to chloroplast deformity, which shows albinism and death phenotypes [28]. *yf* showed yellow leaves due to the deletion mutation of 7-kb, which includes the promoter region and coding sequence of *CsSRP43*. The *CsSRP43* gene encodes a chloroplast signal recognition particle 43 protein [27]. The golden leaf phenotype of C528 is caused by single nucleotide substitution of magnesium chelating enzyme I subunit in *CsChlI* [29]. The *yellow leaf 2.1* (*yl2.1*) mutant, an EMS-induced mutant, exhibited a yellow leaf phenotype. The candidate gene of *yl2.1* encodes a plastid isoform of triosephosphate isomerase (pdTPI) gene [30]. *CsCNGC*, which encodes a cyclic nucleotide gated ion channel protein in cucumber, is the candidate gene of the *v-1* locus in virescent mutant 9110Gt [31]. The spontaneous mutant 104Y, which had virescent leaf phenotype, showed a single nucleotide substitution of *Csa3G890020* gene [32]. SC311Y also exhibited yellow cotyledons and leaves phenotype due to the single-nucleotide polymorphism mutation of *CsVYL* gene [32]. The *CsVYL* gene encodes a DnaJ-like zinc finger protein that plays a key role in plastid development [24]. The appearance of cucumber *ygl* mutant phenotype is caused by the mutation of *tandem 13-lipoxygenase* (*13-LOX*) gene [25]. The *CsHD*, which encodes a histidine and aspartic acid domain containing protein, was considered the candidate gene of *yellow yuong leaf-1* (*yyl-1*) mutant [26]. Although these genes that cause leaf color change have been cloned in cucumber, the molecular mechanism of regulating leaf color is still largely unknown.

In order to further improve the regulation mechanism of leaf color in cucumber, an EMS-induced virescent true leaf mutant *se59* was identified from the wild-type inbred line HB. *CsSE59*, identified by BSA-seq, encodes an INV/PMEIs in cucumber, was the candidate gene for virescent true leaf mutant *se59*. The protein sequence of CsSE59 has 38.67% homology with that of Arabidopsis thaliana, speculating that CsSE59 and its homologues have potentially important functions in chloroplasts. Thus, the results are helpful to clarify the potential function of INV/PMEI in chloroplast development and to understand the detailed regulation mechanism of leaf color variation in cucumber.

2. Materials and Methods

2.1. Plant Materials, Growth Conditions, and Phenotype Identification

A stable heritable mutant *se59* with virescent true leaf was obtained from the EMS-mutagenized wild-type cucumber (the South China type, HB) population, and HB was used as the control. The cucumber plants were planted in a greenhouse with long-day conditions (16-h light/8-h dark, 22–25 °C). The planting substrates contain nutritious soil and vermiculite in the proportion of 1:3 and irrigate the nutrient solution once a week. The light intensity was 305 $\mu mols \cdot m^{-2} \cdot s^{-1}$, and the humidity was 70–85%. The light source was provided by LED lamp. The cotyledon and leaf color of a total of 10 plants began to be observed after seed germination. The plant height, leaf length, leaf width, and petiole length of the third true leaf were measured with a tape. After taking pictures, the area of the third true leaf was measured by ImageJ (V1.8.0) software.

2.2. Genetic Analysis

The F_1, BC_1 and F_2 populations were generated to determine the inheritance pattern of virescent gene (*se59*). After the first true leaf grew up, the variation of the F_2 population were statistically analyzed. The number of plants with wild type and the virescent true leaf phenotype was tested to χ^2 test.

2.3. Photosynthetic Parameter Determination

Transpiration rate and net photosynthetic rate of the true leaves from *se59* mutant and WT plants were measured by CI-340 Handheld Photosynthesis System (Produced by

CID, Camas, WA, USA). The absorption of carbon dioxide refers to the net photosynthetic rate. Three leaves with similar growth and same leaf position of *se59* and wild type were measured from 9:00–11:00 a.m. on a sunny day.

2.4. Measurement of Chlorophyll Fluorescence Kinetic Parameters

Before the determination, the third true leaf of *se59* and wild type were wrapped in tin foil and treated for 30 min in dark. The initial fluorescence (F_0), Fv/Fm, Y (II), qP, NPQ and ETR of each plant were strictly determined according to the operation instructions of chlorophyll fluorescence dynamic parameter instrument MINI-PAM-II (WALZ, Effeltrich, Germany). The leaves of each type of plant were repeated 3 times, and the average value was taken during analysis.

2.5. Measurement of Pigment Contents

The chlorophyll (Chla and Chlb), total chlorophyll (Chl) and carotenoid (Caro) contents were measured at the same development conditions [33]. For chlorophyll extraction, the fresh leaves from the first true leaf in *se59* and HB were picked. Then, 200 mg leaves were put into 15 mL tubes containing 10 mL acetone-ethanol-ddH_2O mixture (volume ratio 4.5:4.5:1) for two days in the dark. After centrifugation, the supernatant was collected, and the contents of Chla, Chlb and Caro were determined by UV-vis spectrophotometer (UV-6800, 7G, China) at absorbance values of 665, 649 and 470 nm, respectively. Chl and Caro were calculated with the following formula: Chla = $(13.95 \times OD_{665} - 6.88 \times OD_{649}) \times V/(1000 \times W)$; Chlb = $(24.96 \times OD_{649} - 7.32 \times OD_{665}) \times V/(1000 \times W)$; Chl = $(6.63 \times OD_{665} + 18.08 \times OD_{649}) \times V/(1000 \times W)$; Caro = $(1000 \times OD_{470} - 2851.304 \times OD_{649} + 811.7385 \times OD_{665})/245$. V: volume of extraction solution, W: sample weight.

2.6. Transmission Electron Microscopy Observation

The first true leaves of 2-week-old wild type and *se59* mutant plants were cut into 2 mm × 2 mm cubes and placed in PBS fixed solution containing 3.5% glutaraldehyde. The leaves were suspended below the liquid level by vacuum treatment and fixed overnight at 4 °C. The leaves were rinsed with PBS buffer and fixed with 1% Osmic acid. After rinsing with PBS buffer, the samples were dehydrated with 30%, 50%, 70%, 80%, 90%, 100% acetone in turn. After that, they were immersed and embedded in Spur's medium, the preparation of ultrathin sections were carried out with Leica EM UC7, and the observation of ultrathin sections were carried out with Hitachi S-3500N scanning electron microscope.

2.7. BSA-Seq Analysis of se59 Locus

For BSA-seq analysis, a *se59* mutant pool (virescent pool) and wild type-like pool (green pool) were collected from F_2 plants according to precise phenotypic collection. 30 of each F_2 individuals were mixed to the same amount to form virescent pool and green pool, respectively. The resulting two pools and two parental pools (*se59* and HB) were constructed and sequenced individually on the Illumina PE150 platform. SNP and InDel of multiple samples were detected by unified genotyping module in GATK3.8 software, and Variant Filtration was used to filter the population vcf file [34]. Using ANNOVAR (V1.1.0) software to annotate the variation site, the genes and variation types of the variation sites were given [35]. This was followed by selecting the variation sites of homozygous differences in parents, taking one of the parents as a reference, calculating the index value of the two offspring pools, respectively, and then calculating the average index of each window to locate the candidate interval.

2.8. RNA-Seq Analysis

For RNA-seq, the first true leaves of wild type and *se59* plants were harvested, respectively. The MiniBEST Plant RNA extraction Kit (Takara) was used to extract the total RNA of each biological replicate. Each sample used 1 μg RNA for library preparation. After the cluster formation, a total of 6 samples were measured using DNBSEQ platform,

and each sample produced an average of 6.44 Gb data. Filter the data using SOAPnuke (BGI, Shanghai, China). First, removal of reads containing adapters; second, removal of reads with unknown base N content greater than 5%; third, removal of low-quality reads. The clean reads were then compared to the reference genome. The HISAT (V2.1.0) (Hierarchical Indexing for Spliced Alignment of Transcripts) software was used to compare reference genomes. Bowtie2 (V2.4.4) software was used to compare clean reads to the reference gene sequence, and then RSEM (V1.3.1) software was used to calculate the expression level of genes and transcripts. Transcripts with minimal 2-fold change in expression ($| \log^2$ FC (fold change) $| \geq 1$) and adjust false discovery rate (FDR) ≤ 0.05 were differentially expressed genes (DEGs).

2.9. RNA Extraction and qRT-PCR

Total RNA of leaf, root and stem were extracted using MiniBEST plant RNA extraction kit (TaKaRa). Total cDNA was obtained using M-MLV (RNase H2) reverse transcriptase (TaKaRa). Quantitative real-time PCR (qRT-PCR) was carried out with the Roche LightCycler 480 (LC480) system using Universal SYBR Green qPCR Premix (ShareBio). The relative expression level of target genes was calculated by $2^{-\Delta\Delta Ct}$ method, and *EFIA* as the internal reference gene [36]. The primers are presented in Table S4.

2.10. Statistical Analysis

Values were represented as means ± SD, and three biological replicates were used for statistical analysis by using SPSS 20.0 (SPSS, Chicago, IL, USA). The statistical significance is determined as $p < 0.05$.

3. Results

3.1. The se59 Produced a Virescent Leaf Phenotype

To further explore and study the function of leaf color-related genes in cucumber, many mutant lines have been obtained by EMS-mediated mutagenesis. We screened several leaf color mutants. One of the mutants, named *se59*, showed a phenotype that has never been reported. Compared with the wild type (HB), the first true leaf of *se59* exhibited virescent leaf color. With an increase in the number of true leaves, the older true leaves gradually turned green until they completely returned to normal green leaf color (Figure 1A–C). However, there was no significant difference in cotyledon color between *se59* mutant and wild type (Figure 1A). In addition, compared with the green fruit color of wild type, the fruit of *se59* also showed a virescent fruit phenotype (Figure 1D).

There is not only a significant difference in true leaf color between *se59* and wild type, but also in other agronomic characters. As shown in Table S1, the plant height of *se59* at cotyledon stage was significantly higher than that of wild type, but at extension stage, *se59* was significantly lower than that of wild type. *se59* was higher than wild type in leaf width, leaf length and petiole length, but there was no significant difference in stem diameter, petal length and petal width (Table S1).

Figure 1. The phenotype virescent leaf mutant *se59* in cucumber. (**A**) True leaf and cotyledon color of the *se59* and WT at the second true leaf stage. Bars = 5 cm. (**B**) True leaf color of the *se59* and WT at the second true leaf stage. Bar = 5 cm. (**C**) Plant of the *se59* and WT at the vine growth stage. Bars = 15 cm. (**D**) Fruit color of *se59* and WT bars = 10 cm.

3.2. Genetic Analysis of se59 Locus

The virescent leaf mutant *se59* was crossed with a green-leaf plant HB to produce F_1, BC_1 and F_2 populations in order to analyze the inheritance of virescent leaf traits. The true leaves of F_1 plants returned to normal green. The plants with virescent true leaf phenotype were isolated from the F_2 population. According to the statistics, 46 plants exhibited virescent true leaf phenotype and 143 plants exhibited normal green true leaf phenotype in F_2 population. The result of χ^2 test ($\chi^2 = 0.044$, $p = 0.83$) showed that the ratio of wild phenotypic plants to variegation phenotypic plants in F_2 generation was 3:1 (WT:*se59* = 143:46). Among the 156 BC_1 plants obtained by crossing F_1 with *se59*, 80 plants were green true leaves and 76 plants were virescent leaves, which accorded with the segregation ratio of 1:1 (Table S2). Thus, we suggested that the virescent phenotype of *se59* mutant was controlled by a single recessive gene.

3.3. The se59 Has Defective Chloroplast Development, Chlorophyll Synthesis and Photosynthetic Capacity at Early Leaf Stage

The morphology of chloroplast in the mesophyll cell of first true leaf of wild type and *se59* mutant have been observed by transmission electron microscopy (TEM) to investigate whether the exhibition of virescent leaf phenotype of *se59* was related to the development of chloroplast. The results showed that the distribution of chloroplasts, thylakoids and starch grains of wild type were uniform (Figure 2A,C), while the chloroplast structure of

se59 mutant was abnormal, such as loose grana lamella, unclear membrane structure and decrease in starch grains. (Figure 2B,D).

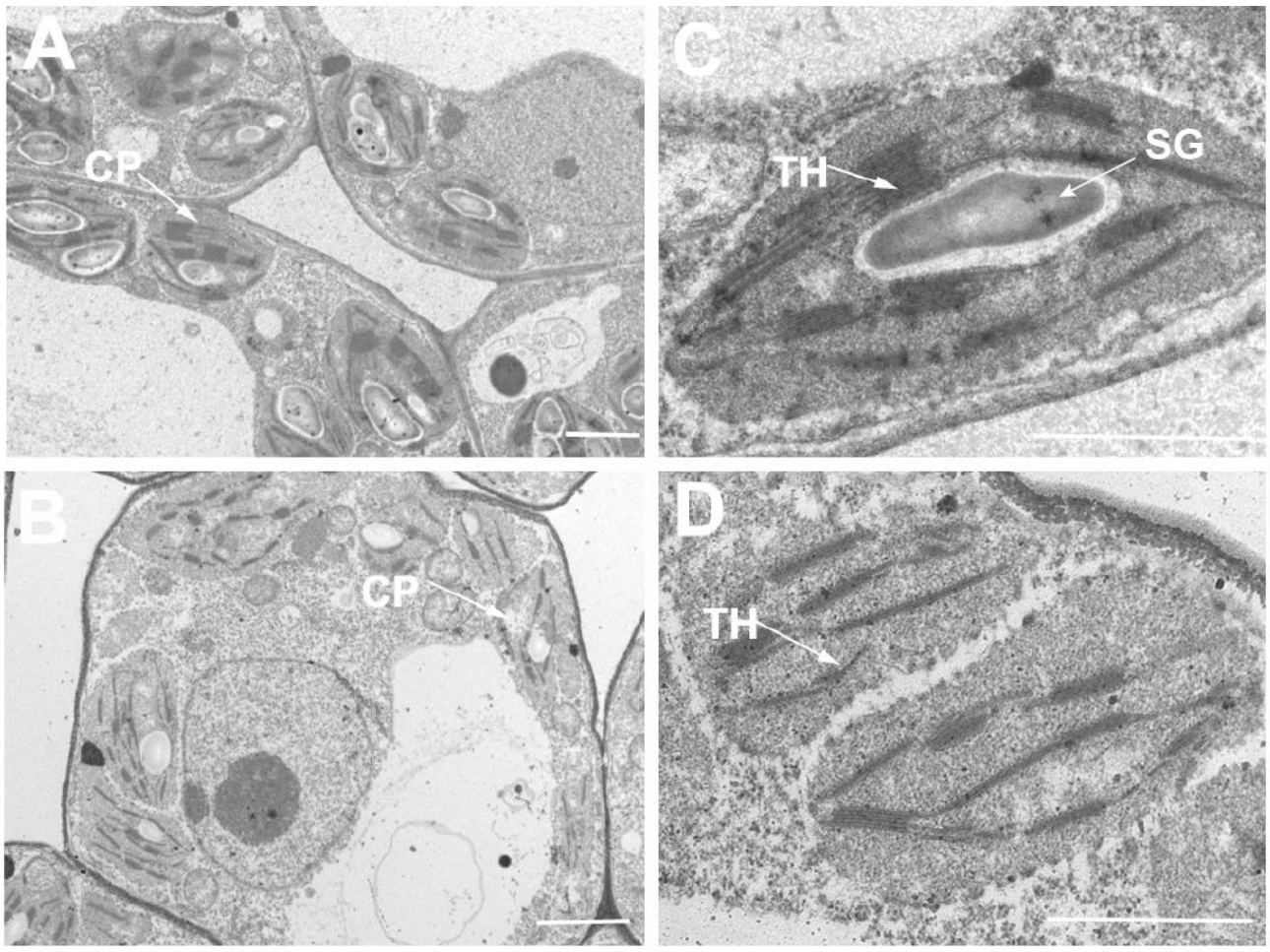

Figure 2. Chloroplast ultrastructure of *se59* and WT. Chloroplast structure of WT (**A**,**C**) and *se59* (**B**,**D**). CP = chloroplast; SG = starch grain; TH = thylakoid. Scale bars = 2 μm.

To investigate whether abnormal chloroplast morphology affects chlorophyll synthesis, the contents of photosynthetic pigments in wild type and *se59* mutant were determined. As shown in Figure 3, at seedling stage, the contents of chlorophyll a, chlorophyll b, total chlorophyll and carotenoid in *se59* mutant were 74%, 82%, 77% and 88% of wild type, respectively. At vine growth stage, the contents of chlorophyll a, chlorophyll b, total chlorophyll and carotenoid in *se59* mutant were 44%, 59%, 50% and 58% of wild type, respectively. These results show that the photosynthetic pigment content of *se59* mutant decreased, but the ability of chloroplast to synthesize chlorophyll was not completely lost.

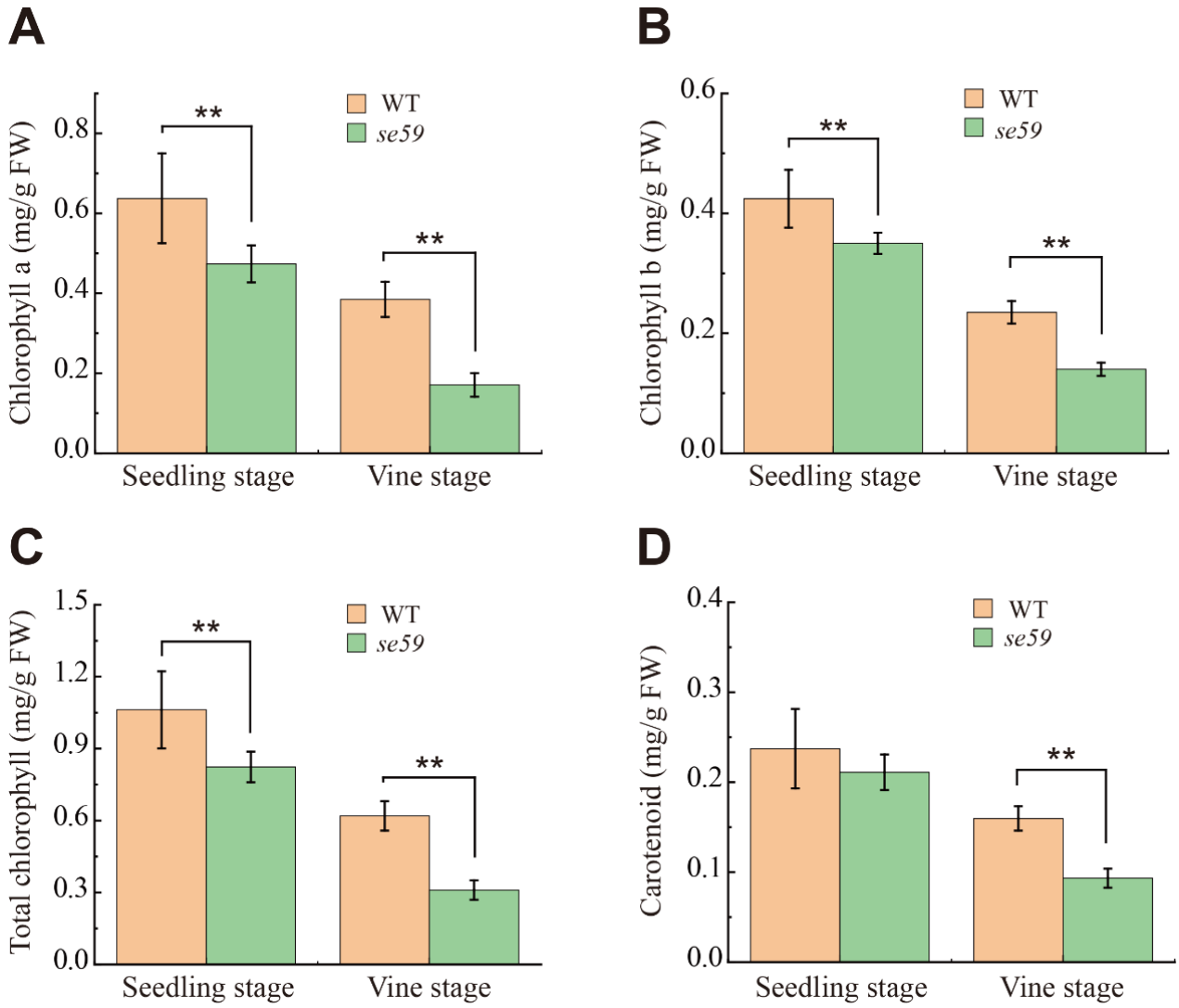

Figure 3. Comparison of pigment contents of the first true leaf of *se59* and WT in cucumber. Content of chlorophyll a (**A**); chlorophyll b (**B**); total chlorophyll (**C**); carotenoid (**D**) in *se59* and WT. ** $p < 0.01$ (*t*-test compared to wild-type values).

To confirm whether the photosynthetic efficiency of *se59* mutant changed, the net photosynthetic efficiency (Pn) and transpiration rate (Tr) of the first true leaf of *se59* and wild type were measured, respectively. As shown in Table 1, compared with the wild type, Pn of *se59* decreased by 34% but Tr was not significantly changed (Table 1). These results indicate that the photosynthetic efficiency of *se59* mutant was significantly affected by the abnormal chloroplast development and the decrease in pigment contents in the mutant.

Table 1. Photosynthetic characteristics of *se59* in cucumber.

Material	Pn (μm/m^2·s)	Tr (μm/m^2·s)
HB	30.07 ± 2.3	3.3 ± 3.4
se59	19.8 ± 4.49 *	5.93 ± 0.46

Note: *: significant difference at $p < 0.05$ by *t*-test.

To explore whether the change of leaf color of the mutant affected the dynamic parameters of chlorophyll fluorescence of *se59* and wild type, the fluorescence dynamic parameters were measured in this study. As shown in Table 2, the non-photochemical

quenching coefficient (NPQ) of *se59* was significantly higher than that of the wild type, but the other parameters were not changed, such as Fv/Fm, Y (II) and ETR (Table 2), indicating that the *se59* mutant may maintain relatively normal photosynthesis by dissipating too much heat.

Table 2. Analysis of fluorescence dynamic parameters of *se59* and wild type (HB) plants during vine growth stage.

Material	F_0	Fv/Fm	Y (II)	qP	NPQ	ETR
HB	416 ± 34.6	0.71 ± 0.06	0.60 ± 0.02	0.83 ± 0.3	0.06 ± 0.08	11.1 ± 0.4
se59	403 ± 6.81	0.67 ± 0.01	0.53 ± 0.47	0.79 ± 0.5	0.18 ± 0.01 *	9.8 ± 0. 8

Note: *: significant difference at $p < 0.05$ by *t*-test.

3.4. Identification of Candidate Genes for se59 Mutant

To determine the genomic region of virescent gene *se59*, The DNA pools of 30 F_2 plants showing virescent leaf phenotype (mutant pool) and 30 F_2 plants showing normal green leaf phenotype (green pool) were re-sequenced. A total of 243,139 pool-specific SNPs were detected in *se59* mutant. By calculating SNP index, the distribution map of SNP loci on seven chromosomes of cucumber was drawn (Figure 4A). Candidate SNPs were selected in accordance with the following criteria: first, SNP-index is equal to 1; second, mutations should be from G to A or from C to T, which are typical EMS mutagenized types; third, the mutation occurs in the mutant but not in the wild type; fourth, the mutation should be located on the exon with non-synonymous mutation or on the alternative splicing site of the intron. Only one SNP (SNP 12112564) with an SNP-index of one was screened (Table 3). SNP 12112564 was located on the first exon of *CsaV3_3G016210* with a nonsynonymous amino acid change. *CsaV3_3G016210* encodes a Invertase/Pectin Methyl Esterase Inhibitor (INV/PMEI). These results demonstrate that *CsaV3_3G016210*, which contains SNP 12112564, is a candidate gene of *se59* mutant in cucumber. In this study, the candidate gene of cucumber virescent leaf mutant was named *CsSE59*.

Table 3. Analysis of the candidate SNP for the *se59* mutant.

Chromo-Some	Position	Gene	Reference	Alteration	SNP_index	Type	Amino Acid Change
Chr.6	12112564	*CsaV3_3G 016210*	G	A	1	exon	G to S

3.5. Sequence and Expression Analysis of CsSE59 Gene

The length of *CsSE59* gene is 10,099 bp and contains two exons and one intron. The coding sequence is 879 bp (Figure 4B). A transition from glycine (Gly) to serine (Ser) at the 61th amino acid occurred in the first exon of *CsSE59* gene due to a G to A substitution (Figure 4B).

To detect the change of *CsSE59* expression in *se59* mutant, the relative expression level of *SE59* was calculated by qRT-PCR. The results show that the expression of *CsSE59* in the mutant was not changed to the wild type (Figure 5A). In addition, *CsSE59* was highly expressed in stem, root and leaf (Figure 5B).

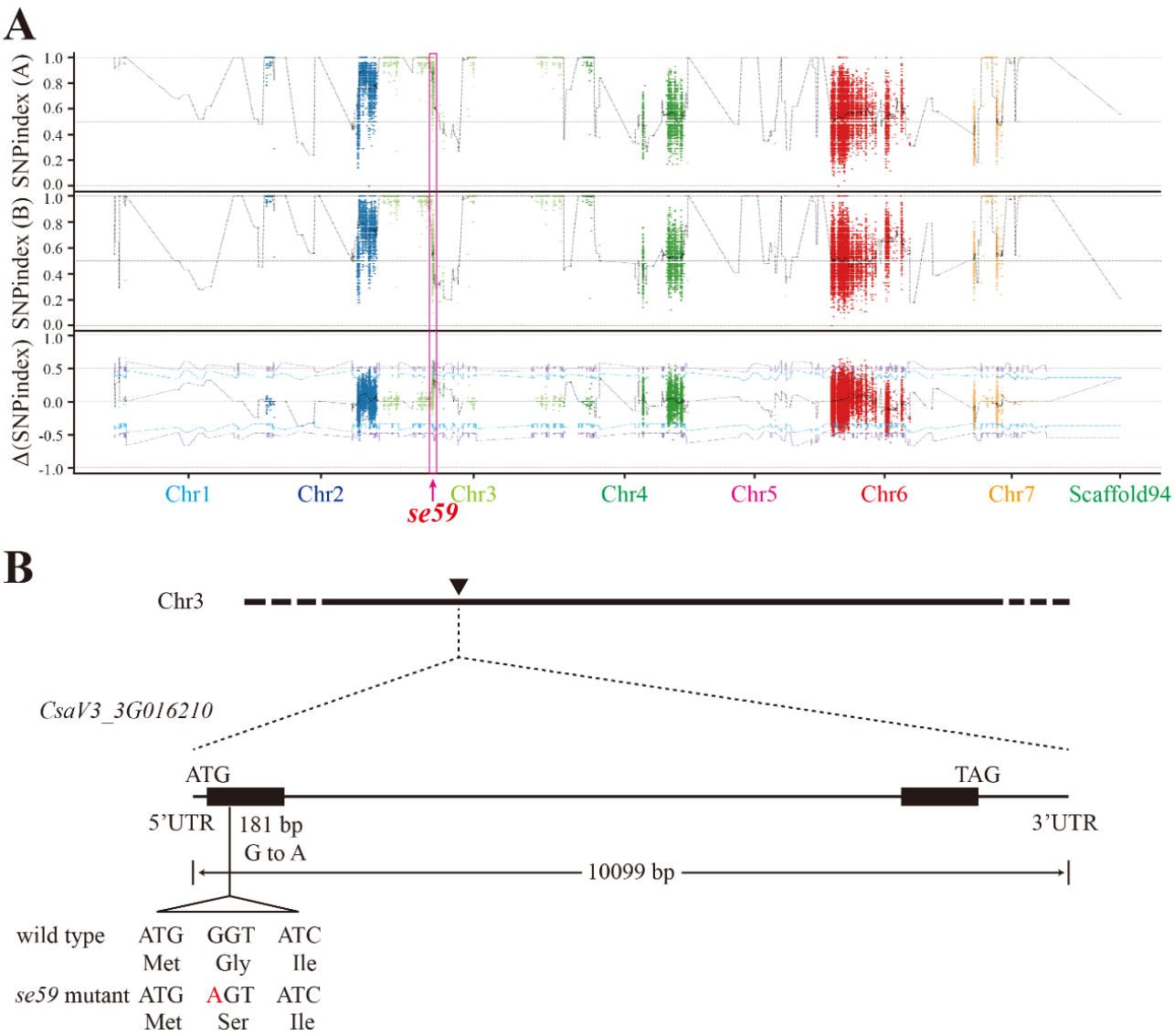

Figure 4. BSA−seq for mapping virescent leaf locus and the structure diagram of *CsSE59* gene. (**A**) Black lines represent SNP_index graph, blue lines indicate the values at 95% ($p < 0.05$), purple lines indicate the values at 99% confidence ($p < 0.01$), red box represents the target genomic region controlling virescent leaf. (**B**) The SNP 12112564 located on cucumber chromosome 3 and the structure of candidate *CsaV3_3G016210*. Solid lines represent introns; rectangles represent exons. The mutated base in the *se59* mutant have been marked in red.

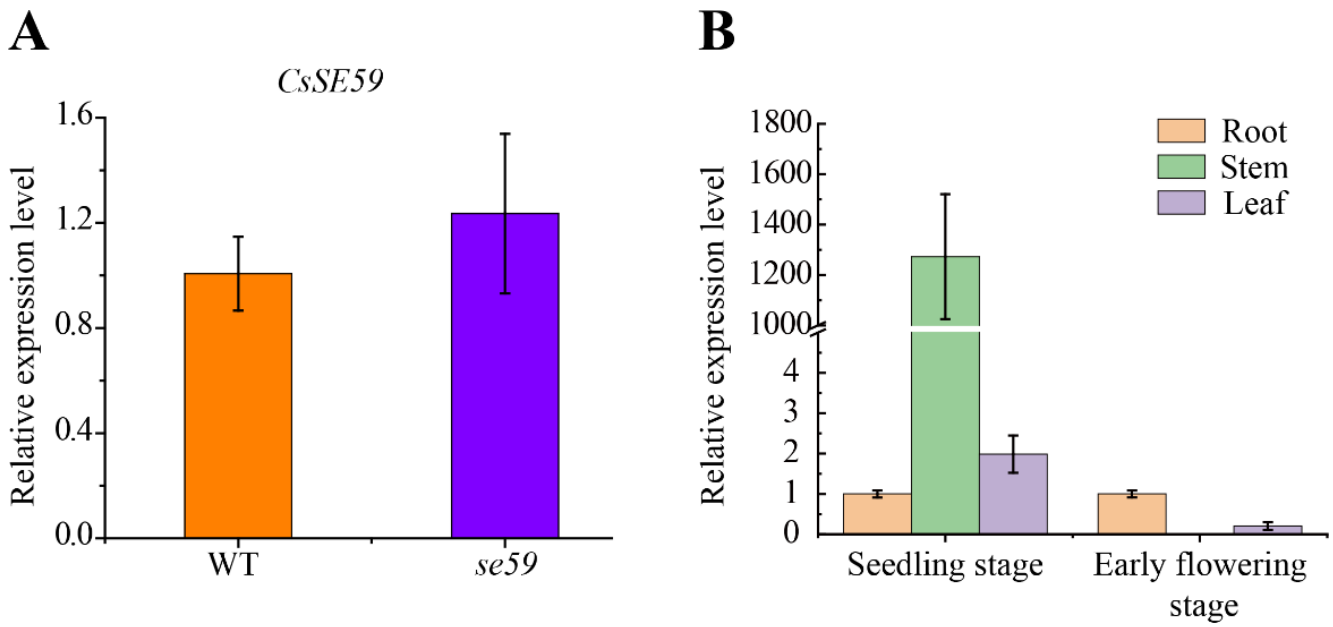

Figure 5. The expression of *CsSE59* in cucumber. (**A**) The relative expression level of *CsSE59* in the first true leaf of WT and *se59* mutant; (**B**) The relative expression level of *CsSE59* in root, stem and leaf of WT plant. The results represent the means ± SD.

3.6. Comparative Transcriptome Analysis between se59 Mutant and Wild Type

To reveal the possible molecular mechanism of virescent leaf formation, the first true leaves of *se59* plant and HB plant were analyzed by RNA-seq. To verify the accuracy of RNA-seq analysis, the expression profiles of 17 cucumber genes were analyzed by qRT-PCR. The data showed that the expression patterns of qRT-PCR and RNA-seq are the same, and there was a good Pearson correlation, indicating that the result of RNA-seq was reliable (Table S3).

According to the screening criteria of DEGs (differentially expressed genes), we found that the total number of DEGs between wild type and *se59* was 923, of which 484 were up-regulated and 439 were down-regulated (Figure S1). The GO annotations and functional classifications indicated that these DEGs were mainly enriched in cellular anatomical entity and intracellular in the cellular component category, catalytic activity and binding in the molecular function category and cellular process in the biological process category (Figure 6A). The GO enrichment analysis showed that these DEGs were mainly enriched in chloroplast, photosynthesis and photosystem (Figure S2). The KEGG pathway enrichment analysis also showed that these DEGs were mainly enriched in photosynthesis and photosynthesis-antenna proteins (Figure 6B). Moreover, DEGs were also enriched in carbon fixation in photosynthetic organisms, biosynthesis of amino acids and carbon metabolism (Figure 6B).

Based on known function and functional predictions, 17 differentially expressed candidate important genes related to virescent leaf phenotype in cucumber were selected (Table S3). Identified by qRT-PCR, among the 17 candidate genes that may be involved in *se59* leaf color phenotype in cucumber, 12 genes were significantly differentially expressed between wild type and mutant. As shown in Figure 7, four genes including *CsaV3_3G012890*, *CsaV3_3G01524038*, *CsaV3_6G004820* and *CsaV3_4G037030* were up-regulated (Figure 7A), while eight genes including *CsaV3_1G032510*, *CsaV3_3G031580*, *CsaV3_4G033870*, *CsaV3_3G005070*, *CsaV3_1G011510*, *CsaV3_6G001010*, *CsaV3_2G009680* and *CsaV3_2G010090* were down-regulated in *se59* (Figure 7B).

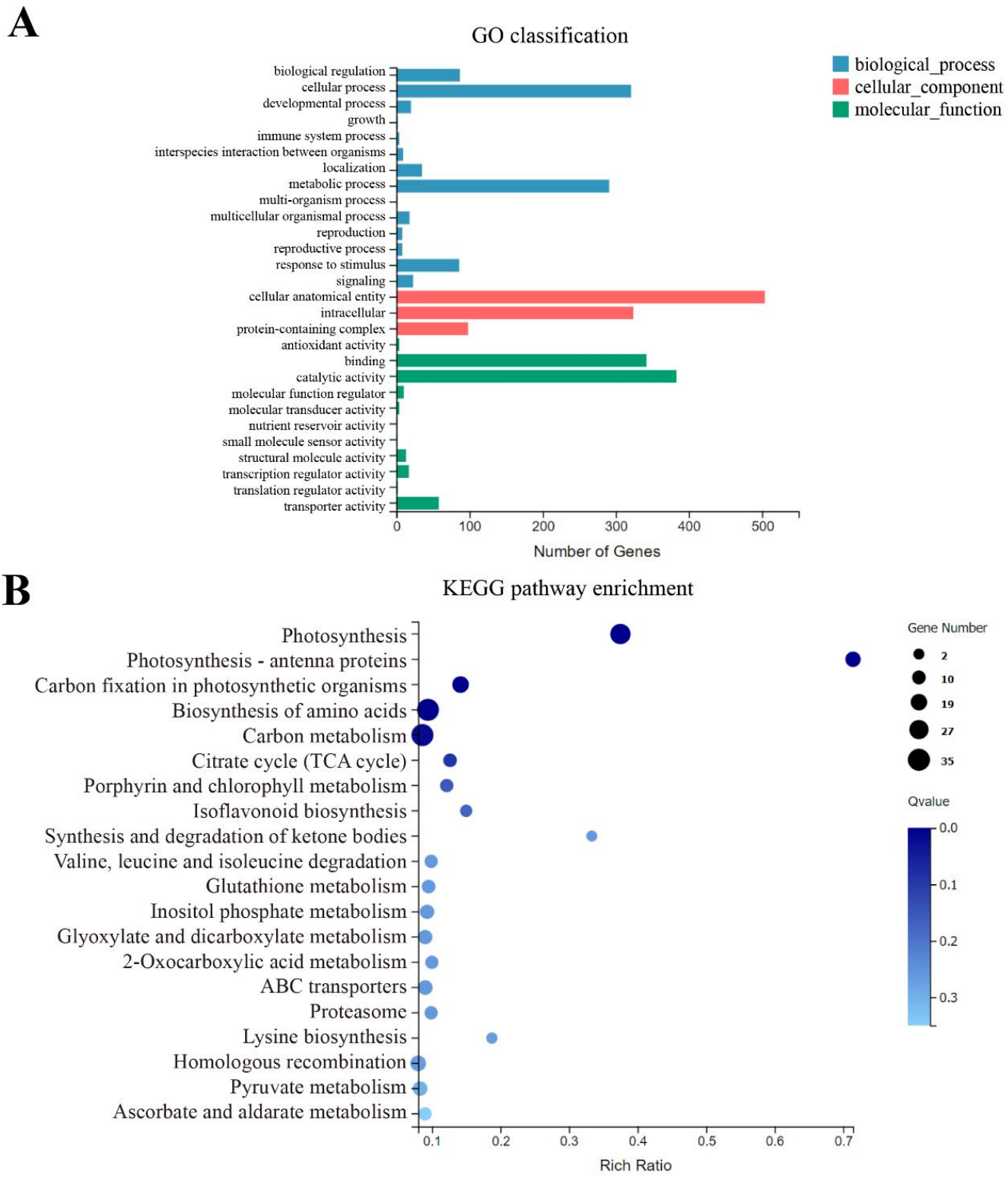

Figure 6. The analysis of GO classification and KEGG pathway enrichment of virescent leaf-related genes in cucumber. (**A**) The GO classification of virescent leaf responsive genes in cucumber; (**B**) The KEGG pathway enrichment scatter plot of virescent leaf-related genes in cucumber.

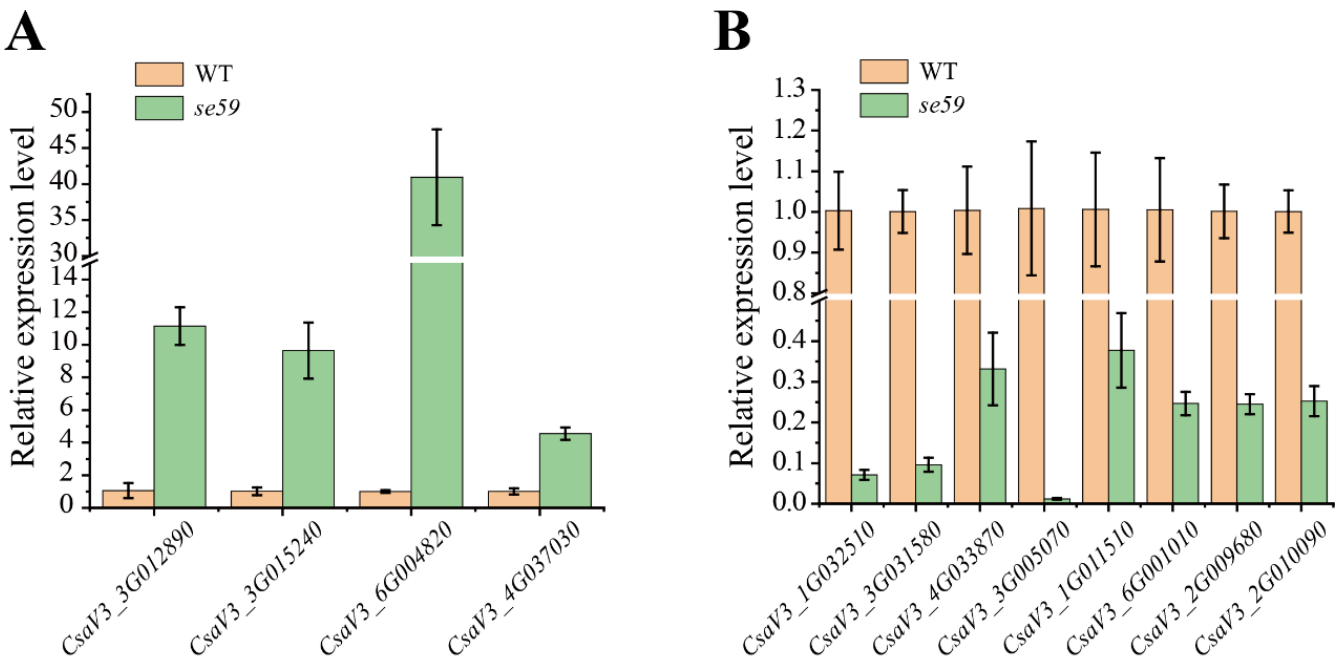

Figure 7. Relative expression levels of 12 virescent leaf-related genes in the first true leaf of *se59* and WT by qRT-PCR analysis. Relative expression levels of four up-regulated genes (**A**) and eight down-regulated genes (**B**) in the first true leaf of *se59* and WT.

4. Discussion

The characteristics of cucumber, such as low natural mutation rate, narrow genetic basis and weak genetic transformation technology, make it difficult for researchers to use T-DNA insertion technology to create cucumber mutants, so there are few reports about cucumber leaf color mutants. To date, a total of 19 leaf color mutants have been reported in cucumber, but only 6 yellow-green leaf mutants have been well characterized [17,24–27,31]. In this study, the cotyledons of *se59* were green before senescence, and the true leaves and veins were yellow-green when each new young leaf emerged. With the development of true leaves, the old true leaves slowly turned green, and *se59* maintained this color conversion process throughout the growth period. At present, no similar phenotype has been reported in cucumber. Therefore, it is speculated that *se59* is a new virescent leaf mutant in cucumber. The appearance of this unique phenotype also indicates that there are some differences in the regulatory mechanisms related to leaf color between cucumber cotyledons and true leaves.

In this study, the virescent mutant *se59* was crossed with green-leaf plant HB to produce F_1, BC_1 and F_2 populations to analyze the inheritance of virescent leaf traits. The true leaves of F1 plants returned to normal green. The ratio of wild phenotypic plants to variegation phenotypic plants in F2 generation was 3:1, showing that the green leaf trait was completely dominant to the yellow leaf trait. Thus, the virescent leaf trait in *se59* was controlled by one single recessive nuclear gene.

Studies have shown that the change of photosynthetic pigment content will change the color of plant leaves. In this study, the chlorophyll content of *se59* was significantly lower than that of the wild type, so we speculated that the leaf yellowing of *se59* was probably due to the decrease in chlorophyll content in *se59* leaves. Photosynthetic pigments have direct or indirect effects on the photosynthetic capacity of plants, which are reflected in the transpiration rate, net photosynthetic rate and other indexes. The net photosynthetic rate of *se59* was significantly lower than that of the wild type, but there was no significant difference in transpiration rate, indicating that the lower photosynthetic capacity of *se59* may be due to the decrease in chlorophyll content affecting plant photosynthesis. However,

Jeknins et al. reported that photosynthesis was not directly related to the significant decrease in chlorophyll content in the maize leaf color mutants [37]. Studies on leaf color mutants of rice and wheat also showed that there was no significant relationship between chlorophyll content and photosynthetic rate [38,39]. Other studies have shown that the decrease in photosynthetic ability will lead to the decrease in organic matter accumulated by the plant, which makes the plant grow weakly, explaining the reason why the *se59* plant is slightly shorter than the wild type.

CsaV3_3G016210, the only candidate gene for the *se59* locus, encodes a predicted INV/PMEI. INV/PMEI is a large protein superfamily that participated in the tight post-transcriptional regulation of INVs and PMEs. These two classes of enzymes have different enzyme activities in carbohydrate metabolism [40]. INVs play different roles in organ development, carbohydrate distribution, sugar signaling and response to biotic and abiotic stresses [40–43]. INVs contains acid INVs and neutral/alkaline INVs, which exhibit different pH optima and subcellular localizations. The optimum PH of acid INVs is 3.5–5.0. It can be divided in vacuolar and cell wall INVs. The optimum PH of neutral/alkaline INVs is 6.8–9.0, which is located in plastids, mitochondrion, cytosol and nucleus. INV inhibitor (INVI) can regulate the INV activity. Currently, little is known about their roles in plant physiology [44–46]. The deduced protein sequence of CsSE59 has 38.67% homology with its *Arabidopsis thaliana* homolog, which is predicted to be located in plastid, indicating that CsSE59 and its homologs have a potentially important function in chloroplast. Taken together, *se59* impaired chloroplast development and chlorophyll biosynthesis, resulting in etiolated seedlings. This study provides clues for further studying the role of *CsSE59* in chloroplast development and exploring the molecular mechanism of this leaf color variation. Next, we will examine whether the leaf color phenotype of *se59* mutants is only caused by *CsSE59* mutation by transgenic supplement experiments, and try to reveal the molecular mechanism of *CsSE59* regulating chloroplast development and chlorophyll synthesis.

5. Conclusions

In this study, we reported an EMS-induced mutant *se59*. The *se59* mutant showed the phenotype of virescent true leaves, while the cotyledon color was normal. The chloroplast development of *se59* mutant was defective, and its photosynthetic pigment content decreased significantly, resulting in a significant decrease in its photosynthetic ability. The results of RNA-seq analysis showed that the DEGs were mainly enriched in photosynthesis and photosynthesis-antenna proteins. BSA-seq results showed that *CsSE59* (*CsaV3_3G016210*), which encodes an Invertase/Pectin Methyl Esterase Inhibitor (INV/PMEI), were the only candidate gene. The expression levels of *CsSE59* were high in leaves and stems. Overall, the results of this study will help to deepen the understanding of the regulatory mechanism related to leaf color change in cucumber.

Supplementary Materials: The following supporting information can be downloaded at: https://www.mdpi.com/article/10.3390/horticulturae9090951/s1, Figure S1: Volcanic map of differences between groups of *se59* and WT; Figure S2: The GO enrichment scatter plot of virescent leaf related genes in cucumber; Table S1: Agronomic properties of wild type and mutant *se59* at different growth periods; Table S2: The separation ratio of normal leaf color and virescent leaf traits of BC1 and F2 generations; Table S3: Candidate differentially expressed genes related to leaf color; Table S4: Primers used in qRT-PCR.

Author Contributions: Conceptualization, S.L. and Y.Z. (Yuelong Zhou); Methodology, L.L. (Liting Liao) and L.X.; Software, L.L. (Liu Liu), Z.Z. and Z.H.; Validation, Y.Z. (Yong Zhou), L.L. (Liting Liao), L.L. (Liu Liu) and Z.Z.; Formal analysis, L.L. (Liting Liao), L.L. (Liu Liu) and Z.H.; Data curation, Y.Z. (Yong Zhou), L.L. (Liting Liao), L.L. (Liu Liu), L.X., Z.Z. and Z.H.; Writing—original draft preparation, Y.Z. (Yuelong Zhou); Writing—review and editing, Y.Z. (Yuelong Zhou) and S.L.; Supervision, Z.Z.; Project administration, S.L.; funding acquisition, S.L. All authors have read and agreed to the published version of the manuscript.

Funding: This research was funded by the National Natural Science Foundation of China (32160709), the Academic and Technical Leader Plan of Jiangxi Provincial Main Disciplines (20204BCJ22023), the earmarked fund for Innovation team of Jiangxi Agricultural University (JXAUCXTD009), and the Natural Science Fund project in Jiangxi province (20232BAB205013).

Data Availability Statement: Not applicable.

Conflicts of Interest: The authors declare no conflict of interest.

References

1. Mao, G.; Wei, H.; Hu, W.; Ma, Q.; Zhang, M.; Wang, H.; Yu, S. Fine mapping and molecular characterization of the virescent gene *vsp* in Upland cotton (*Gossypium hirsutum*). *Theor. Appl. Genet.* **2019**, *132*, 2069–2086. [CrossRef]
2. Chen, N.; Wang, P.; Li, C.; Wang, Q.; Pan, J.; Xiao, F.; Wang, Y.; Zhang, K.; Li, C.; Yang, B.; et al. A Single Nucleotide Mutation of the *IspE* Gene Participating in the MEP Pathway for Isoprenoid Biosynthesis Causes a Green-Revertible Yellow Leaf Phenotype in Rice. *Plant Cell Physiol.* **2018**, *59*, 1905–1917. [CrossRef] [PubMed]
3. Deng, X.J.; Zhang, H.Q.; Wang, Y.; He, F.; Liu, J.L.; Xiao, X.; Shu, Z.F.; Li, W.; Wang, G.H. Mapped clone and functional analysis of leaf-color gene *Ygl7* in a rice hybrid (*Oryza sativa* L. ssp. indica). *PLoS ONE* **2014**, *9*, e99564. [CrossRef] [PubMed]
4. Waters, B.M.; Chu, H.-H.; DiDonato, R.J.; Roberts, L.A.; Eisley, R.B.; Lahner, B.; Salt, D.E.; Walker, E.L. Mutations in Arabidopsis yellow stripe-like1 and yellow stripe-like3 reveal their roles in metal ion homeostasis and loading of metal ions in seeds. *Plant Physiol.* **2006**, *141*, 1446–1458. [CrossRef] [PubMed]
5. Zhang, L.; Liu, C.; An, X.; Wu, H.; Feng, Y.; Wang, H.; Sun, D. Identification and genetic mapping of a novel incompletely dominant yellow leaf color gene, *Y1718*, on chromosome 2BS in wheat. *Euphytica* **2017**, *213*, 141. [CrossRef]
6. Marco, G.D.; Giardi, M.T.; Massacci, A.; Tricoli, D. Photosynthetic properties of leaves of a yellow green mutant of wheat compared to its wild type. *Photosynth Res.* **1989**, *21*, 117–122. [CrossRef] [PubMed]
7. Barry, C.S.; Mcquinn, R.P.; Chung, M.Y.; Besuden, A.; Giovannoni, J.J. Amino acid substitutions in homologs of the STAY-GREEN protein are responsible for the green-flesh and chlorophyll retainer mutations of tomato and pepper. *Plant Physiol.* **2008**, *147*, 179–187. [CrossRef]
8. Nothnagel, P.S. Inheritance and mapping of a yellow leaf mutant of carrot (Daucus carota). *Plant Breed.* **2003**, *122*, 339–342. [CrossRef]
9. Zou, J.J.; Singh, R.J.; Hymowitz, T. Association of the yellow leaf (y10) mutant to soybean chromosome 3. *J. Hered.* **2003**, *94*, 352–355. [CrossRef]
10. Pasini, L.; Bruschini, S.; Bertoli, A.; Mazza, R.; Fracheboud, Y.; Marocco, A. Photosynthetic performance of cold-sensitive mutants of maize at low temperature. *Physiol. Plant.* **2005**, *124*, 362–370. [CrossRef]
11. Park, S.Y.; Yu, J.W.; Park, J.S.; Li, J.; Yoo, S.C.; Lee, N.Y.; Lee, S.K.; Jeong, S.W.; Seo, H.S.; Koh, H.J.; et al. The senescence-induced staygreen protein regulates chlorophyll degradation. *Plant Cell* **2007**, *19*, 1649–1664. [CrossRef]
12. Ma, X.; Sun, X.; Li, C.; Huan, R.; Sun, C.; Wang, Y.; Xiao, F.; Wang, Q.; Chen, P.; Ma, F.; et al. Map-based cloning and characterization of the novel yellow-green leaf gene ys83 in rice (*Oryza sativa*). *Plant Physiol. Biochem.* **2017**, *111*, 1–9. [CrossRef] [PubMed]
13. Gong, X.; Jiang, Q.; Xu, J.; Zhang, J.; Teng, S.; Lin, D.; Dong, Y. Disruption of the rice plastid ribosomal protein s20 leads to chloroplast developmental defects and seedling lethality. *G3 (Bethesda)* **2013**, *3*, 1769–1777. [CrossRef] [PubMed]
14. Wu, Z.; Zhang, X.; He, B. A chlorophyll-deficient rice mutant with impaired chlorophyllide esterification in chlorophyll biosynthesis. *Plant Physiol.* **2007**, *145*, 29–40. [CrossRef] [PubMed]
15. Zhao, C.; Xu, J.; Chen, Y.; Mao, C.; Zhang, S.; Bai, Y.; Jiang, D.; Wu, P. Molecular cloning and characterization of OsCHR4, a rice chromatin-remodeling factor required for early chloroplast development in adaxial mesophyll. *Planta* **2012**, *236*, 1165–1176. [CrossRef]
16. Cui, X.; Wang, Y.; Wu, J.; Han, X.; Gu, X.; Lu, T.; Zhang, Z. The RNA editing factor DUA1 is crucial to chloroplast development at low temperature in rice. *New Phytol.* **2019**, *221*, 834–849. [CrossRef]
17. Zhang, K.; Li, Y.; Zhu, W.; Wei, Y.; Njogu, M.K.; Lou, Q.; Li, J.; Chen, J. Fine Mapping and Transcriptome Analysis of Virescent Leaf Gene *v-2* in Cucumber (*Cucumis sativus* L.). *Front. Plant Sci.* **2020**, *11*, 570817. [CrossRef]
18. Sugimoto, H.; Kusumi, K.; Tozawa, Y.; Yazaki, J.; Kishimoto, N.; Kikuchi, S.; Iba, K. The virescent-2 mutation inhibits translation of plastid transcripts for the plastid genetic system at an early stage of chloroplast differentiation. *Plant Cell Physiol.* **2004**, *45*, 985–996. [CrossRef]
19. Sugimoto, H.; Kusumi, K.; Noguchi, K.; Yano, M.; Yoshimura, A.; Iba, K. The rice nuclear gene, *VIRESCENT 2*, is essential for chloroplast development and encodes a novel type of guanylate kinase targeted to plastids and mitochondria. *Plant J.* **2007**, *52*, 512–527. [CrossRef]
20. Yoo, S.C.; Cho, S.H.; Sugimoto, H. Rice virescent3 and stripe1 encoding the large and small subunits of ribonucleotide reductase are required for chloroplast biogenesis during early leaf development. *Plant Physiol.* **2009**, *150*, 388–401. [CrossRef]
21. Kusumi, K.; Sakata, C.; Nakamura, T. A plastid protein NUS1 is essential for build-up of the genetic system for early chloroplast development under cold stress conditions. *Plant J.* **2011**, *68*, 1039–1050. [CrossRef] [PubMed]

22. Zhang, Q.; Xue, D.; Li, X.; Long, Y.; Zeng, X.; Liu, Y. Characterization and molecular mapping of a new virescent mutant in rice. *J. Genet. Genom.* **2014**, *41*, 353–356. [CrossRef] [PubMed]
23. Qi, Y.; Liu, X.; Liang, S.; Wang, R.; Li, Y.; Zhao, J.; Shao, J.; An, L.; Yu, F. A Putative Chloroplast Thylakoid Metalloprotease VIRESCENT3 Regulates Chloroplast Development in Arabidopsis thaliana. *J. Biol. Chem.* **2016**, *291*, 3319–3332. [CrossRef] [PubMed]
24. Song, M.; Wei, Q.; Wang, J. Fine Mapping of CsVYL, Conferring Virescent Leaf through the Regulation of Chloroplast Development in Cucumber. *Front. Plant Sci.* **2018**, *9*, 432. [CrossRef]
25. Ding, Y.; Yang, W.; Su, C.; Ma, H.; Pan, Y.; Zhang, X.; Li, J. Tandem 13-Lipoxygenase Genes in a Cluster Confers Yellow-Green Leaf in Cucumber. *Int. J. Mol. Sci.* **2019**, *20*, 3102. [CrossRef] [PubMed]
26. Hu, L.; Zhang, H.; Xie, C.; Wang, J.; Zhang, J.; Wang, H.; Weng, Y.; Chen, P.; Li, Y. A mutation in *CsHD* encoding a histidine and aspartic acid domain-containing protein leads to *yellow young leaf-1* (*yyl-1*) in cucumber (*Cucumis sativus* L.). *Plant Sci.* **2020**, *293*, 110407. [CrossRef]
27. Zhang, T.; Dong, X.; Yuan, X. Identification and characterization of CsSRP43, a major gene controlling leaf yellowing in cucumber. *Hortic. Res.* **2022**, *9*, 212. [CrossRef]
28. Ke, X.; Shen, J.; Niu, Y. Cucumber NUCLEAR FACTOR-YC2/-YC9 target translocon component CsTIC21 in chloroplast photomorphogenesis. *Plant Physiol.* **2023**, *192*, 2822–2837. [CrossRef]
29. Gao, M.; Hu, L.; Li, Y.; Weng, Y. The chlorophyll-deficient golden leaf mutation in cucumber is due to a single nucleotide substitution in CsChlI for magnesium chelatase I subunit. *Theor. Appl. Genet.* **2016**, *129*, 1961–1973. [CrossRef]
30. Xiong, L.; Du, H.; Zhang, K. A Mutation in CsYL2.1 Encoding a Plastid Isoform of Triose Phosphate Isomerase Leads to Yellow Leaf 2.1 (yl2.1) in Cucumber (*Cucumis sativus* L.). *Int. J. Mol. Sci.* **2020**, *22*, 322. [CrossRef]
31. Miao, H.; Zhang, S.; Wang, M.; Wang, Y.; Weng, Y.; Gu, X. Fine Mapping of Virescent Leaf Gene *v-1* in Cucumber (*Cucumis sativus* L.). *Int. J. Mol. Sci.* **2016**, *17*, 1602. [CrossRef] [PubMed]
32. Zhang, Z.; Wang, J.; Xing, G.; Li, M.; Li, S. Integrating physiology, genetics, and transcriptome to decipher a new thermo-sensitive and light-sensitive virescent leaf gene mutant in cucumber. *Front. Plant Sci.* **2022**, *13*, 972620. [CrossRef] [PubMed]
33. Tang, Y.; Wang, R. Change Law of Hyperspectral Data in Related with Chlorophyll and Carotenoid in Rice at Different Developmental Stages. *Rice Science* **2004**, *11*, 274–282.
34. Abe, A.; Kosugi, S.; Yoshida, K.; Natsume, S.; Takagi, H.; Kanzaki, H.; Matsumura, H.; Yoshida, K.; Mitsuoka, C.; Tamiru, M.; et al. Genome sequencing reveals agronomically important loci in rice using MutMap. *Nat. Biotechnol.* **2012**, *30*, 174–178. [CrossRef]
35. Takagi, H.; Abe, A.; Yoshida, K.; Kosugi, S.; Natsume, S.; Mitsuoka, C.; Uemura, A.; Utsushi, H.; Tamiru, M.; Takuno, S.; et al. QTL-seq: Rapid mapping of quantitative trait loci in rice by whole genome resequencing of DNA from two bulked populations. *Plant J.* **2013**, *74*, 174–183. [CrossRef] [PubMed]
36. Livak, K.J.; Schmittgen, T.D. Analysis of Relative Gene Expression Data Using Real-Time Quantitative PCR and the $2-\Delta\Delta CT$ Method. *Methods* **2001**, *25*, 402–408. [CrossRef]
37. Jenkins, C.L. Effects of the Phosphoenolpyruvate Carboxylase Inhibitor 3,3-Dichloro-2-(Dihydroxyphosphinoylmethyl) propenoate on Photosynthesis: C(4) Selectivity and Studies on C(4) Photosynthesis. *Plant Physiol.* **1989**, *89*, 1231–1237. [CrossRef]
38. Fischer, R.A.; Rees, D.; Sayre, K.D.; Lu, Z.M.; Condon, A.G.; Saavedra, A.L. Wheat yield progress associated with higher stomatal conductance and photosynthetic rate, and cooler canopies. *Crop Sci.* **1998**, *38*, 1467–1475. [CrossRef]
39. Zhou, X.S.; Xing, W.D.; Quan, S.S. High photosynthetic efficiency of a rice (*Oryza sativa* L.) xantha mutant. *Photosynthetica* **2006**, *44*, 316–319. [CrossRef]
40. Gough, J.; Karplus, K.; Hughey, R.; Chothia, C. Assignment of homology to genome sequences using a library of hidden Markov models that represent all proteins of known structure. *J. Mol. Biol.* **2001**, *313*, 903–919. [CrossRef]
41. Ruan, Y.L.; Jin, Y.; Yang, Y.J.; Li, G.J.; Boyer, J.S. Sugar input, metabolism, and signaling mediated by invertase: Roles in development, yield potential, and response to drought and heat. *Mol. Plant* **2010**, *3*, 942–955. [CrossRef] [PubMed]
42. Tauzin, A.S.; Giardina, T. Sucrose and invertases, a part of the plant defense response to the biotic stresses. *Front. Plant Sci.* **2014**, *5*, 293. [CrossRef] [PubMed]
43. Liao, S.; Wang, L.; Li, J.; Ruan, Y.L. Cell wall invertase is essential for ovule development through sugar signaling rather Than provision of carbon nutrients. *Plant Physiol.* **2020**, *183*, 1126–1144. [CrossRef] [PubMed]
44. Bate, N.J.; Niu, X.; Wang, Y.; Reimann, K.S.; Helentjaris, T.G. An invertase inhibitor from maize localizes to the embryo surrounding region during early kernel development. *Plant Physiol.* **2014**, *134*, 246–254. [CrossRef] [PubMed]
45. Raiola, A.; Camardella, L.; Giovane, A. Two Arabidopsis thaliana genes encode functional pectin methylesterase inhibitors11The industrial utilization of Arabidopsis and kiwi PMEIs is patent pending it, no. RM2003A000346. *FEBS Lett.* **2004**, *557*, 199–203. [CrossRef]
46. Lionetti, V. PECTOPLATE: The simultaneous phenotyping of pectin methylesterases, pectinases, and oligogalacturonides in plants during biotic stresses. *Front. Plant Sci.* **2015**, *6*, 331. [CrossRef]